ISTFA™ 2009, Conference Proceedings from the
35th International Symposium for Testing and Failure Analysis
November 15–19, 2009, San Jose, California, USA, p 162-165

# Failure Analysis of Breakdown Sites in Silicon Solar Cells

***Otwin Breitenstein, Jan Bauer, Jan-Martin Wagner, Horst Blumtritt, Nikolai Zakharov***
*Max Planck Institute of Microstructure Physics, Halle, Germany*
*breiten@mpi-halle.mpg.de, +49-345-5582740*

***Andriy Lotnyk***
*Christian-Albrecht-University, Kiel, Germany*

## Abstract

In this contribution the use of electroluminescence imaging, bias-dependent lock-in thermography, special dark and illuminated lock-in thermography techniques, and electron microscopy techniques is demonstrated for investigating the physical mechanism of breakdown in multicrystalline silicon solar cells. Two dominant breakdown mechanisms are identified, which are breakdown at recombination-active crystal defects, showing a relatively soft breakdown, and avalanche breakdown at dislocation-induced etch pits, which occurs very steep (hard breakdown) and dominates in our cells at high reverse bias.

## Introduction

In a solar module about 36 cells are connected in series in so-called strings. The current flowing through all cells is the same, but the cell biases are floating. Only if all cells have the same illuminated current-voltage (*I-V*) characteristics, they are all operating at the same working point and their generated voltages simply add up. However, if one of these cells should be shadowed or broken, leading to a reduced photocurrent of this cell, the other cells may bias this one in reverse direction to up to -18 V. If then a large reverse current flows, which may be as large as the short circuit current of the other cells (typically 7 A), this cell dissipates a lot of heat and the module may be destroyed thermally. According to its base doping concentration of $10^{16}$ cm$^{-3}$, a solar cell should undergo avalanche breakdown at -60 V. However, in reality breakdown may occur already at -10 to -15 V. Therefore the electric breakdown behavior of solar cells is an important reliability aspect and must be studied in detail.

The two breakdown mechanisms discussed in literature are avalanche breakdown (impact ionization) and internal field emission (Zener breakdown) [1]. Avalanche breakdown is the generation of electron-hole pairs by the impact of accelerated carriers. It is characterized by the multiplication of photocurrents in the breakdown sites. It shows a negative temperature coefficient (TC) of the current for a fixed bias, since at high temperature phonon scattering quenches the impact efficiency. Zener breakdown, on the other hand, is direct tunneling of carriers through the energy gap. It shows no multiplication of photo-induced carriers and its TC is positive, since the gap shrinks with increasing temperature. This mechanism is more probable than avalanche only at high doping concentrations above $10^{18}$ cm$^{-3}$, where the breakdown voltage is in the order of -6 V. The probability of all breakdown mechanisms increases with increasing net doping concentration. For a base doping concentration of $10^{16}$ cm$^{-3}$ as in our solar cells, breakdown should occur by avalanche at voltages beyond -60 V. However, it is well-known that local breakdown may occur already at lower reverse bias if the p-n junction is not flat but curved, leading to a local increase of the electric field.

In this investigation the dominant breakdown sites in industrial multicrystalline Si solar cells are localized by lock-in thermography (LIT) under reverse bias. Special LIT techniques allow us to image the temperature coefficient, the slope (steepness) of the breakdown current variation with voltage, and the avalanche multiplication factor locally. The distribution of grown-in recombination-active crystal defects is obtained by electroluminescence (EL) imaging. By using different electron microscopy techniques, the physical origin of the dominating breakdown mechanism in the investigated cells is identified.

## Results

### Typical Breakdown Characteristics

Fig. 1 shows the reverse dark current-voltage characteristic of the investigated cell at two temperatures. For this investigation a typical 156x156 mm$^2$ sized industrially produced solar cell made from solar-grade multicrystalline silicon was selected, which was free of significant ohmic shunts. Weak (soft) breakdown starts already at -6 V and hard breakdown occurs beyond -13 V. As Fig. 1 shows, in the hard breakdown regime the current shows a negative temperature coefficient (TC), as it is known from avalanche breakdown, whereas in the soft breakdown regime (below -13 V) the TC is positive. Already this observation points to the presence of different breakdown mechanisms acting in different bias ranges.

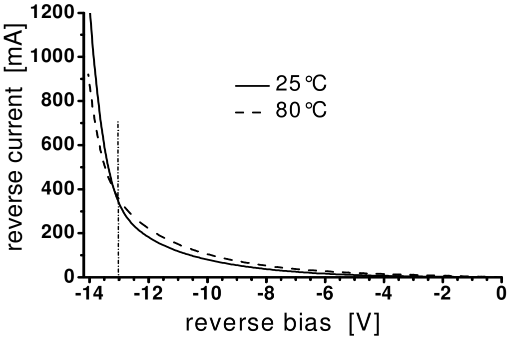

*Figure 1: Reverse bias I-V characteristic of the investigated cell at two temperatures.*

### Electroluminescence Imaging and Bias-Dependent Lock-in Thermography

In the forward-bias electroluminescence (EL) image Fig. 2 (a) regions containing recombination-active crystal defects are visible as dark areas, which are mainly grain boundaries and dislocations. Four interesting regions are labeled by 'A', 'B', 'C', and 'D'. In lock-in thermography (LIT) the locally dissipated heat in a device is imaged [2]. The two LIT images Fig. 2 (b) and (c), taken at reverse biases of -12 and -15 V, show that at different biases different breakdown sites dominate. At -12 V (b) the breakdown sites strongly correlate with dark regions of recombination-active defects in (a), see e.g. in regions 'A' and 'B'. It can be noted that, on the average, in regions with a strong dark EL contrast also stronger breakdown occurs and vice versa. At -15 V, however, new breakdown sites appear in regions without recombination-active defects, see regions 'C' and 'D'. Note that Fig. 2 (c) is scaled very insensitively, hence the currents in (c) are much higher than in (b).

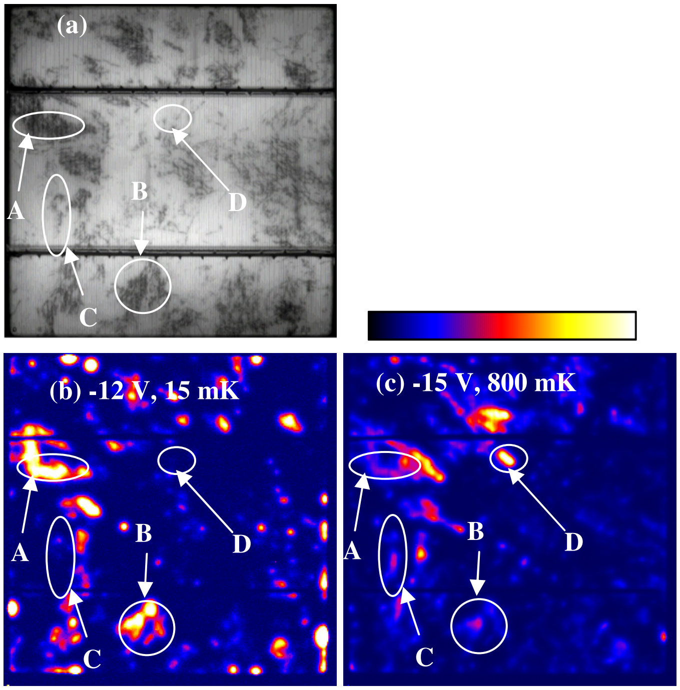

*Figure 2: (a) Forward-bias EL image of this cell, (b) reverse-bias LIT image at -12 V, (c) reverse-bias LIT image at -15 V. Note the different scaling ranges in (b) and (c).*

### Imaging Physical Breakdown Parameters

If the LIT signal being -90° phase shifted to the bias pulses is displayed and the cell has no series resistance problems, the LIT signal is a quantitative measure of the locally flowing current density and can be scaled in units of mA/cm$^2$ [2]. Then, by subtracting two current density images taken at different biases at the same temperature, or at different temperatures at the same bias, respectively, and dividing by the bias / temperature difference, images of the local bias-dependence (slope) or of the local temperature coefficient (TC) of the local current can be obtained. Since these values are still dependent on the absolute magnitude of the current flowing, it is useful to relate them to the mean values of the local currents. In this way images of the relative slope (steepness, given in % current change per Volt) and the relative TC (given in % current change per Kelvin) are obtained, which allow to image the basic physical parameters of breakdown sites quantitatively [3].

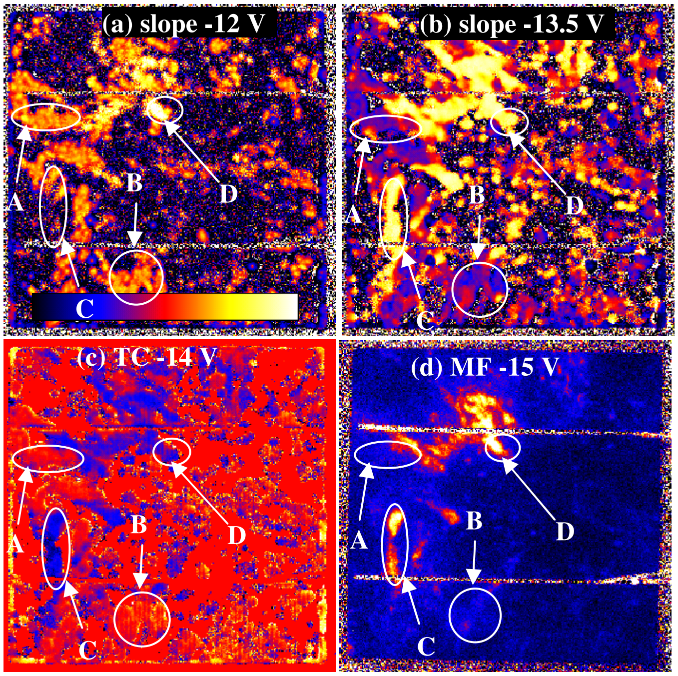

*Figure 3: (a) Slope at -12 V, scaled from 0 to 100 %/V, (b) slope at -13.5 V, scaled from 0 to 150 %/V, (c) temperature coefficient, measured at -14 V, scaled from -3 %/K to +3 %/K, (d) avalanche multiplication factor at -15 V, scaled from 1 to 3. (a), (b) taken at 60 °C, (c) at 70 °C. (d) at room temperature.*

Fig. 3 (a) shows such a slope image belonging to a bias of -12 V, scaled from 0 (black) to 100 %/V (white, see color bar). This image again correlates well with the EL image Fig. 2 (a) in that regions 'A' and 'B' appear bright. Note that at this bias the breakdown site 'C' is not visible yet but site 'D' is. Fig. 3 (b) shows a slope image belonging to a higher bias of -13.5 V, scaled to 150 %/V. Here also the site 'C' appears, but 'A' and 'B' appear relatively weaker, since their slope is lower (soft breakdown). In the TC image Fig. 3 (c) taken at -14 V all sites of steep breakdown (e.g. 'C' and 'D') appear dark, hence they show a negative TC. However, breakdown sites 'A' and 'B' show a close-to-zero TC (red), hence here obviously another breakdown mechanism is active. This becomes obvious in Fig. 3 (d) which shows the local avalanche multiplication factor (MF) at -15 V, scaled from MF = 1 to 3. For obtaining this image, the bias of -15 V was permanently applied to the cell and the cell was illuminated homogeneously in a pulsed manner. Then the lock-in signal is a measure of the locally flowing photocurrent and also can be scaled in units of mA/cm$^2$. Note that the dark breakdown current, which is visible in Fig. 2 (b) and (c), does not influence this photocurrent image, since it is steady-state. It turns out that, at reverse biases between zero and -13 V, the photocurrent image is nearly homogeneous, but at higher reverse bias regions of avalanche multiplication appear bright. By dividing the photocurrent image taken at a certain bias $V$ (here -15 V) to one taken at a lower bias (here -13 V), a quantitative local image of the avalanche multiplication factor MF at bias $V$ can be obtained [3]. The MF image Fig. 3 (d) shows that only the regions with the steepest slope at -13.5 V (e.g. 'C' and 'D') show significant avalanche multiplication, but the regions of defect-induced breakdown (e.g. 'A' and 'B') do not.

**Electron Microscopy**

The question is: What are the different physical mechanisms of breakdown in these different regions? For answering this question, scanning electron microscopy (SEM) has been applied at the interesting sites, including lock-in EBIC (electron beam-induced current) imaging under high reverse bias [4]. For this investigation only lock-in EBIC is appropriate, which is working with a pulsed beam and an a.c.-coupled current amplifier, since any d.c.-coupled amplifier would be overloaded by the strong steady-state breakdown current. While in regions 'A' and 'B' nothing special could be seen, in region 'C' at a reverse bias above -13 V lines and spots of bright EBIC signal appear, see Fig. 4 (a). Such sites are traditionally called microplasma sites. In these regions field-induced avalanche multiplication of beam-generated minority carriers occurs. In the SE image Fig. 4 (b) in these sites black spots are visible (see arrows), which in higher magnification (c) can be identified as conical etch pits. Note that this cell was acidically textured, which is standard for modern solar cells since this texturization works independent of crystal orientation. The recipe of this texture is actually chosen to avoid the appearance of etch pits, but obviously some types of defects still generate them.

In Fig. 4 (c) a pair of etch pits is shown which obviously is connected by a planar defect, maybe a stacking fault. The region between the arrows in (c) was processed into a TEM lamella by focused ion beam (FIB) preparation. The resulting TEM image is shown in (d). Here we see that the tips of the etch pits are really sharp (radius about 20 nm) and that they are indeed caused by dislocation-like defects. The exact type of this defect is yet under investigation. Since in these cells the p-n junction is lying about 300 nm below the surface, at these tips the junction should be bowl-shaped with a radius of 300 nm. Sze and Gibbons [5] have calculated the avalanche breakdown voltage for bowl-shaped p-n junctions and have found that, for a net doping concentration of $p = 10^{16}$ cm$^{-3}$ and a radius of 300 nm, the avalanche breakdown voltage indeed reduces from about -60 V (for a flat junction) to -13 V, which was also found by us for breakdown in regions 'C' and 'D'. Hence, by these investigations we have successfully identified the mechanism being responsible for the "hard" breakdown e.g. in regions 'C' and 'D' as an avalanche breakdown, with the field being enhanced by the tip effect at the bottom of the observed etch pits. The measured negative TC of this breakdown current fits to this interpretation. It is understandable that this effect is observed mainly in regions where no high density of recombination-active defects is observed, since for avalanche effect clean material is necessary for enabling a large scattering path length of the carriers.

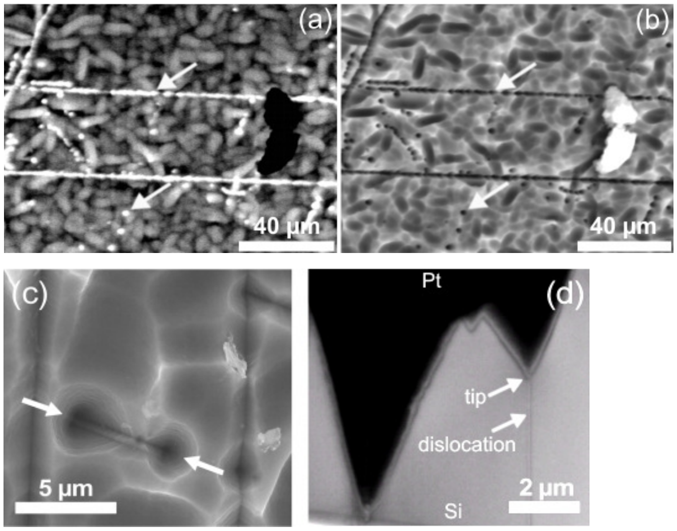

*Figure 4: (a) Lock-in-EBIC image at -15 V in region 'C' showing microplasma sites, (b) corresponding SE image, (c) detailed SE image of single microplasma sites, (d) TEM cross section of this site after FIB preparation between arrows in (c).*

## Discussion and Conclusions

The origin of the defect-induced breakdown e.g. in sites 'A' and 'B' is less clear yet. It has been shown by Lausch et al. [6] that this type of breakdown also occurs at a flat surface. Many authors have discussed the influence of defects like dislocations on the avalanche breakdown voltage, but this influence was meant to be basically due to a field increase by the presence of charged defects. Then also the defect-induced breakdown should show a negative TC and should lead to avalanche multiplication, which, however, was not observed in regions 'A' and 'B'. Therefore, we believe that for this breakdown electronic gap states of the defects are responsible. This hypothesis is supported by our observation that there is a correlation between the recombination activity of these defects and the magnitude of the breakdown current. It was also observed that only weak defect-induced breakdown sites show some 1.55 µm defect-induced luminescence, but strong ones do not [7]. This can be explained by a different degree of contamination of the defects, leading to different densities of deep defect states. One of our hypotheses is that trap-induced tunneling might be the mechanism responsible for defect-induced breakdown. This mechanism is physically related to internal field emission (Zener effect, tunneling through the gap), which is actually improbable at a doping concentration as low as $10^{16}$ $cm^{-3}$. However, if the tunneling occurs not through the whole gap but in two steps via mid-gap states, this mechanism would become much more probable. Actually, as for the Zener effect, we would expect a positive TC for this mechanism, since the gap energy reduces with increasing temperature. However, in Fig. 3 (c) we have measured a close-to-zero TC in regions 'A' and 'B', which is not completely understood yet. Therefore another hypothesis is that the mechanism is a kind of "trap-assisted avalanche". Since a gap level may be occupied either by an electron or a hole, in a trap-assisted avalanche process the impact should lead to subsequent electron and hole emission with a certain delay time in between. This might be the reason why this process shows no significant multiplication of photo-generated carriers. At least it seems to be clear that this defect-induced breakdown becomes stronger with increasing degree of contamination of the defects. Therefore it may become the dominant breakdown mechanism if upgraded metallurgical grade (UMG) material is being used instead of gas-phase purified silicon for solar cells in future.

## Acknowledgments

This work was financially supported by the German Federal Ministry for the Environment, Nature Conservation and Nuclear Safety and all the industry partners within the research cluster SolarFocus (0327650 D). The content of this publication is the responsibility of the authors.

## References

[1] Mahadevan, S., Hardas, S.M., Suryan, G., "Electrical Breakdown in Semiconductors", *Physica Status Solidi (a)* Vol. **8** (1971), pp. 335-374

[2] Breitenstein, O., Langenkamp, M.: Lock-in Thermography - Basics and Use for Functional Diagnostics of Electronic Components, Springer (Berlin / Heidelberg / New York 2003), ISBN 3-540-43439-9

[3] Breitenstein, O., Bauer, J., Wagner, J.-M., Lotnyk, A., "Imaging Physical Parameters of Pre-Breakdown Sites by Lock-in Thermography Techniques", *Prog. Photovolt: Res. Appl.*, Vol. **16** (2008), pp. 679-685

[4] Bauer, J., Wagner, J.-M., Lotnyk, A., Blumtritt, H., Lim, B., Schmidt, J., Breitenstein, O., "Hot spots in multicrystalline silicon solar cells: avalanche breakdown due to etch pits", *Physica Status Solidi RRL* Vol. **3** (2009), pp. 40-42

[5] Sze, S.M., Gibbons, G., "Effect of junction curvature on breakdown voltage in semiconductors", *Solid-State Electronics* Vol. **9** (1966), pp. 831-845

[6] Lausch, D., Petter, K., v. Wenckstern, H. Grundmann, M., "Correlation of Pre-Breakdown Sites and Bulk Defects in Multicrystalline Solar Cells", *Physica Status Solidi RRL*, Vol. **3** (2009), pp. 70-72

[7] O. Breitenstein, J. Bauer, J.-M. Wagner, H. Blumtritt, A. Lotnyk, M. Kasemann, W. Kwapil, W. Warta: Physical mechanisms of breakdown in multicrystalline silicon solar cells, presented at IEEE Photovoltaic Specialists Conference (PVSC), Philadelphia, June 2009, proceedings in preparation.